

Charge-density waves in the mixed-valence two-dimensional metal $K_3Cu_8S_6$

L. W. ter Haar, F. J. Di Salvo,* H. E. Bair, R. M. Fleming, and J. V. Waszczak
AT&T Bell Laboratories, Murray Hill, New Jersey 07974

W. E. Hatfield

Chemistry Department, University of North Carolina at Chapel Hill, Chapel Hill, North Carolina 27514

(Received 27 June 1986)

In order to study the physical properties of $K_3Cu_8S_6$, we have carefully defined the synthetic conditions for KCu_4S_3 , $K_3Cu_8S_6$, and KCu_3S_2 . $K_3Cu_8S_6$ is apparently a kinetic phase and must be trapped with a minimum amount of either KCu_4S_3 or KCu_3S_2 . Magnetic susceptibility and electrical resistivity data display behavior typical of charge-density-wave systems. In view of the low-dimensional metallic nature of $K_3Cu_8S_6$ and preliminary x-ray data, a second-order reversible transition at $T_1 = 152 \pm 1$ K has been identified as the onset of an incommensurate lattice. In the region of 50–60 K, a first-order transition with considerable hysteresis seems to be a structural transition to a commensurate superlattice state.

I. INTRODUCTION

Rudorff *et al.*¹ first reported the existence of the composition $K_3Cu_8S_6$ as part of an investigation concerning the products of high-temperature fusion reactions involving alkali-metal carbonates, copper, and sulfur. Their results indicated that the new phases $Na_2Cu_3S_3$, KCu_4S_3 , $RbCu_4S_3$, and $K_3Cu_8S_6$ all have metallic conductivity at room temperature ($\approx 50\text{--}100 \Omega^{-1} \text{cm}^{-1}$) in addition to a blue-black metallic lustre. Stimulated by the apparent "mixed valency" of the Cu (e.g., Cu^+ and Cu^{2+}) and the electrical conductivity of these compounds, a number of workers have taken a closer look at the structural and physical properties of some of these materials.

The composition " $Na_2Cu_3S_3$ " was reported by Rudorff¹ as the sole product of the fusion reaction between copper, sulfur, and sodium carbonate. More recent results by both Burschka² and Brown³ have shown that this $Na_2Cu_3S_3$ phase is actually $Na_3Cu_4S_4$, and can be described as a one-dimensional metal. The structure consists of one-dimensional columns of $[Cu_4S_4]^{3-}$ chains separated by sodium ions, and the physical properties are in agreement with metallic behavior.

Brown⁴ has also reported single-crystal x-ray diffraction results and physical properties for the KCu_4S_3 phase reported by Rudorff.¹ Their results indicate that KCu_4S_3 adopts a double-layer structure (S-Cu-S-Cu-S) and exhibits metallic behavior. Therefore, KCu_4S_3 is a two-dimensional metal as opposed to the one-dimensional example provided by $Na_3Cu_4S_4$. Burschka⁵ has reported the structure for $CsCu_4S_3$ and found it to be isotypic with KCu_4S_3 and $RbCu_4S_3$.

The first attempts by Burschka to synthesize $K_3Cu_8S_6$ were unsuccessful and led to the discovery of the as yet unknown compound KCu_3S_2 .⁶ Interestingly, Burschka⁵ has also found that $CsCu_3S_2$ exists, but that it adopts a new structure type which is totally unlike that of KCu_3S_2 . In subsequent work, Burschka⁷ succeeded in synthesizing $K_3Cu_8S_6$ and reported the results of a single-crystal x-ray

diffraction study. The synthetic conditions Burschka reported were, however, in conflict with those reported by Rudorff.¹ In a closely related study, Schils *et al.*⁸ reported the synthesis and structure of the isotypic compounds $Rb_3Cu_8Se_6$ and $Cs_3Cu_8Se_6$.

Stimulated by the variety of compounds obtained from this series of alkali-metal carbonate fusion reactions as well as the intriguing combination of unusual structure and metallic conductivity, we have reinvestigated the synthesis of $K_3Cu_8S_6$ in order to investigate its physical properties. Both magnetic susceptibility and electrical resistivity measurements were made, and both show remarkably unusual behavior, behavior which we feel is most likely attributable to the presence of a charge-density wave (CDW).

II. SYNTHESIS

There are three K-Cu-S phases which can be obtained from high-temperature fusion reactions involving K_2CO_3 , powdered copper, and elemental sulfur. Namely, these are KCu_4S_3 (or $K_2Cu_8S_6$), $K_3Cu_8S_6$, and KCu_3S_2 (or $K_3Cu_9S_6$). It is interesting to note at this point the stoichiometric relationship,



since there are also synthetic and structural trends which systematically vary from KCu_4S_3 to KCu_3S_2 . Since there are discrepancies in the literature concerning the syntheses of these materials, we report our synthesis with some detail.

Rudorff¹ first reported that by reacting 6 g potassium carbonate, 6 g sulfur and 1 g copper powder ($K_2CO_3:S:Cu$ in 2.8:1:12 molar ratios), KCu_4S_3 or $K_3Cu_8S_6$ can be obtained. By slowly heating to a specified temperature and soaking at that temperature for a specified time, either KCu_4S_3 (800 °C, 1 h) or $K_3Cu_8S_6$ (1000 °C, 3 h) can be the resultant product. The single-crystal x-ray diffraction study by Brown⁴ demonstrated that KCu_4S_3 can indeed be

synthesized in this manner. However, any systematic attempts to change the procedure in order to improve crystal size or quality, were generally unsuccessful. Burschka⁶ was attempting to synthesize $K_3Cu_8S_6$ by Rudorff's method (1000°C, 3 h) when he discovered the as yet unknown phase, KCu_3S_2 . His final results indicated that KCu_3S_2 was best synthesized in the temperature range 780–850°C with a one-hour soak period. His report simply concluded that at lower temperatures, both KCu_4S_3 and $K_3Cu_8S_6$ could be identified in powder x-ray diffraction patterns, but did not elaborate. In his later study, Burschka⁷ reported that $K_3Cu_8S_6$ was indeed obtainable from a lower, but somewhat narrow temperature range. At 790°C he found that the formation of KCu_4S_3 and/or $K_3Cu_8S_6$ could be controlled by the length of the soak period. Specifically, two hours led to a product which yielded x-ray quality crystals of $K_3Cu_8S_6$.

In our own initial attempts to synthesize $K_3Cu_8S_6$, we actually synthesized several unwanted batches of either KCu_4S_3 or KCu_3S_2 . $K_3Cu_8S_6$ would sometimes appear only as the minor second phase in a few of the multiphase batches. $K_3Cu_8S_6$ crystals are needlelike, and as such, are easy to separate from the layerlike crystals of KCu_4S_3 . On the other hand, KCu_3S_2 crystals are also needlelike and for all practical purposes, indistinguishable from $K_3Cu_8S_6$. So, if a few x-ray-quality-sized crystals is all that is desired, the mixed-phase system of KCu_4S_3 - $K_3Cu_8S_6$ is the system of choice since the two materials can be easily distinguished from one another. However, in order to obtain bulk single-phase $K_3Cu_8S_6$ product, and in order to clarify the discrepancies in the literature, we have attempted to define the syntheses of these materials more precisely.

We initially held to Rudorff's prescribed amounts of starting material (6 g K_2CO_3 , 6 g S, 1 g Cu) since we felt the large excess of potassium and sulfur was necessary to provide a growth medium for the crystals (a hypothesis later verified by experiments discussed below). The starting materials were ground together and placed into an alumina crucible which was deep enough to contain the initial bubbling (foaming) which occurs upon heating. The crucible was covered with a tight fitting alumina cap, and then placed inside a long and deep carbon crucible. This carbon crucible was then placed inside a vertical quartz tube which was contained inside a vertical tube furnace. Without the graphite crucible, K_2CO_3 vapor attacked the quartz tube irreversibly. Provisions at the top of the quartz tube allowed the system to be sealed off with an inert gas flow (argon) and the insertion of a thermocouple down to the reaction zone. The quartz vessel was long enough such that some of it was exposed to room-temperature air in order to keep it cool enough so that excess sulfur would condense on the quartz walls and not inside the gas-glow tubing (where blockage could occur).

After sufficient flushing of the reaction vessel with the argon, a small flow rate of argon (1 bubble/sec in oil bubbler) was maintained throughout the reaction process. Figure 1 is a plot of our synthesis results in terms of set-point temperature versus soak period. The heating rate from room temperature to the set point was 125°C/h. To cool the reaction, the furnace was simply shut off at the end of

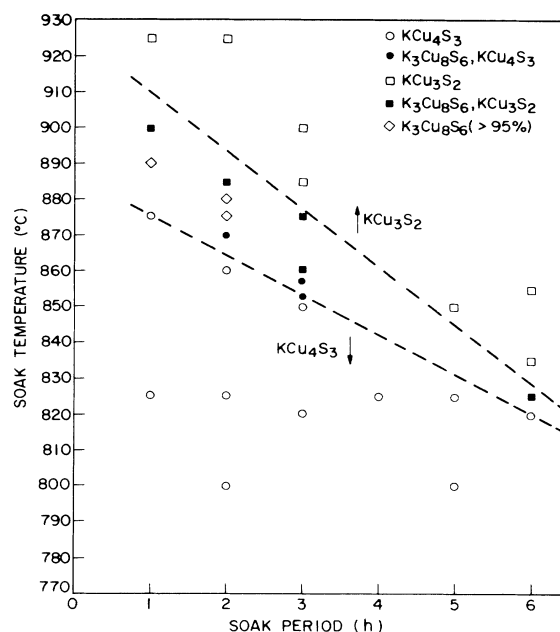


FIG. 1. By plotting the reaction soak period versus soak temperature, the observed trend becomes self-evident. The cleanest $K_3Cu_8S_6$ can be isolated around 875°C and 1–2 h. The area between the two dashed lines indicates the conditions under which at least some $K_3Cu_8S_6$ can be observed along with either KCu_4S_3 or KCu_3S_2 .

the soak period and allowed to cool down at a rate of approximately 125°C/h. Figure 1 demonstrates the relationship we began to notice after several runs. In general, KCu_4S_3 and KCu_3S_2 are the predominant phases in the reaction system. The lower-temperature phase is KCu_4S_3 , and the higher temperature phase is KCu_3S_2 . The boundary between these two phases varies from approximately 900°C to 800°C, depending on the length of the soak period. Clean material of either KCu_4S_3 or KCu_3S_2 can be made by using reaction conditions well removed from the boundary lines as indicated in Fig. 1. In between the boundary lines is where $K_3Cu_8S_6$ can be found as a product. The data in Fig. 1 indicate that a shorter soak period and higher soak temperature favor the formation of $K_3Cu_8S_6$. For soak periods of 5 h or longer, $K_3Cu_8S_6$ is hardly detectable in x-ray powder patterns since the boundary between KCu_4S_3 and KCu_3S_2 apparently becomes more crisply defined. The optimum conditions for synthesizing $K_3Cu_8S_6$ seem to be a soak temperature of 875°C for a 1–2-h period. When soaked for less than one hour, the product is neither crystalline nor clean in terms of its x-ray powder diffraction pattern. Finally, the last parameter which we found to affect the reaction product was the particle size of the K_2CO_3 . The data in Fig. 1 are for well-ground materials. When coarser K_2CO_3 was used, the effective boundary line shifted to a higher temperature and/or a longer time. We interpret this as a result of the kinetics of K_2CO_3 decomposition and its reaction with sulfur. Smaller K_2CO_3 particles simply allow for faster kinetics due to their increased surface area with

respect to larger particles. Since the formation of $K_3Cu_8S_6$ is sensitive towards the reaction time and temperature, it is actually not surprising that the K_2CO_3 particle size would also have a pronounced effect on $K_3Cu_8S_6$ formation. By all evidence, $K_3Cu_8S_6$ seems to be a kinetic phase (i.e., nonequilibrium) and as such, must be "trapped" under the best available conditions. Our cleanest product was greater than $\sim 95\%$ pure $K_3Cu_8S_6$. The small amount of KCu_4S_3 was easily recognizable (platelets) and manually separated from the $K_3Cu_8S_6$ crystals.

The actual workup of the cooled cake is straightforward. Since the cooled cake is usually firmly stuck in the alumina crucible, it is filled with a deoxygenated 50:50 mixture of ethanol and distilled water to leach out the soluble polysulfides. The yellow solution is decanted off after some time is allowed for the leaching to occur (ultrasonic agitation helps), and then the process is repeated. When the solution becomes colorless and odorless, the leaching process is complete and shiny blue-black crystals should be all that remain. After suction filtering the crystals under an argon flow, they are washed with absolute ethanol and anhydrous ethyl ether. The crystals can then be thoroughly dried under vacuum. $K_3Cu_8S_6$ crystals are needlelike crystals that are similar in overall appearance to the KCu_3S_2 crystals. KCu_4S_3 crystals form easily recognizable platelets. If $K_3Cu_8S_6$ crystals are left exposed to the atmosphere, they will lose their metallic lustre over the course of a few days due to oxidation reactions with moist air. Product batches were characterized by powder x-ray diffraction. Powder patterns for the pure materials are displayed in Fig. 2 and demonstrate that mixtures can be easily identified since many diffraction peaks do not overlap between the three phases. The relative purity of product batches was estimated from the diffraction pattern intensities as well as by visible examination in the case of KCu_4S_3 - $K_3Cu_8S_6$ mixtures.

III. RESULTS

A. Magnetism

Magnetic susceptibility data for $K_3Cu_8S_6$ were obtained using a cryogenically equipped Faraday balance at an externally applied magnetic field of 10.6 kG and a gradient of 0.939 kG/cm.⁹ The data are displayed in Fig. 3 using two different formats. The upper curve represents the experimentally observed gram susceptibility. The data were collected with the temperature decreasing as well as with the temperature increasing at rates of 0.5–1.0 K/min. The rising susceptibility at low temperatures in the upper curve is due to a Curie contribution from paramagnetic impurities. Hence, the data below 15 K were fit to the form $\chi_0 + C/(T + \Theta)$, where χ_0 is assumed to be temperature independent and $C/(T + \Theta)$ accounts for the paramagnetic impurity ($C = 3.573$, $\Theta = 0$) and is subtracted out of the entire upper curve in Fig. 3 to yield the lower curve. The lower curve is assumed to be the intrinsic susceptibility and is the sum of the diamagnetic core contributions and the Pauli-Landau and Van-Vleck paramagnetic contributions. The magnetic susceptibility is only weakly temperature dependent above 180 K, but shows a stronger temperature dependence indicative of phase transitions below 180 K. There is a reversible transition (probably second order) at approximately 150 K which is more clearly displayed in the derivative $d\chi_g/dT$ as shown in Fig. 4. The curve for $d\chi_g/dT$ is obtained by fitting the observed χ_g data to a quadratic polynomial for every eight consecutive data points. The linear coefficient is then extracted and plotted versus temperature to yield the $d\chi_g/dT$ versus T curve. In the region of 50 K there is a first-order transition with considerable hysteresis. A pretransition "dip" in the susceptibility appears at about 60–65 K in the cooling curves, but not in the heating curve.

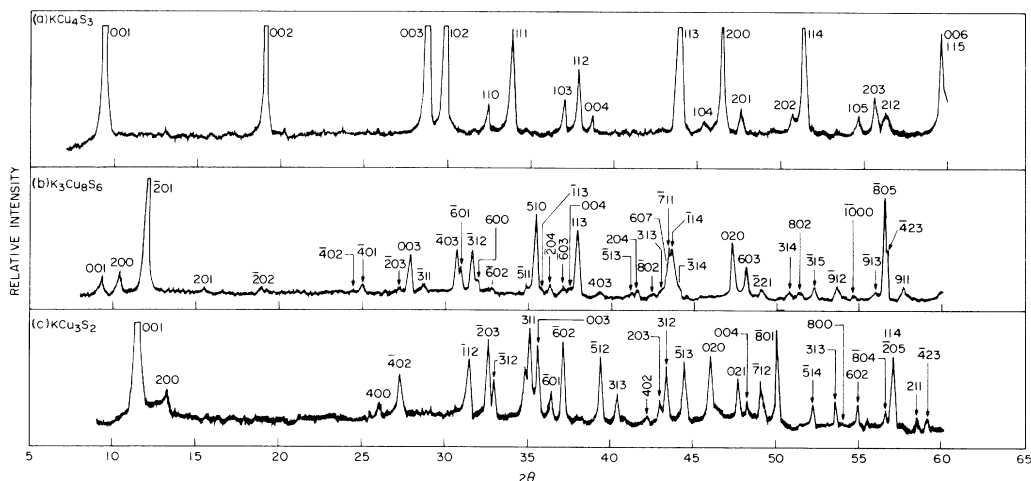


FIG. 2. Powder x-ray diffraction patterns for KCu_4S_3 , $K_3Cu_8S_6$, and KCu_3S_2 . KCu_4S_3 : tetragonal, $a = 3.899$ Å, $c = 9.262$ Å. $K_3Cu_8S_6$: monoclinic, $a = 17.332$ Å, $b = 3.83$ Å, $c = 9.889$ Å, $\beta = 104.12^\circ$. KCu_3S_2 : monoclinic, $a = 14.773$ Å, $b = 3.946$ Å, $c = 8.182$ Å, $\beta = 113.5^\circ$.

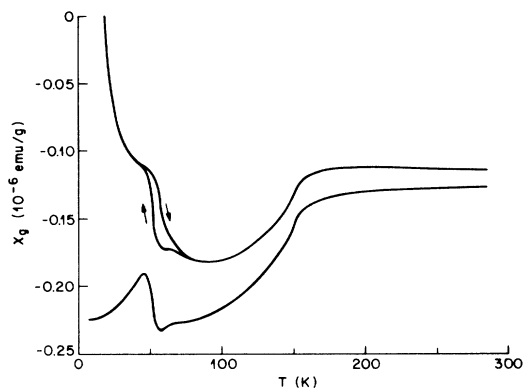


FIG. 3. Magnetic susceptibility data for $K_3Cu_8S_6$. Upper curve is the experimentally observed data during cooling and heating. The lower curve is the cooling data minus an impurity Curie term.

B. Conductivity

Temperature-dependent electrical-resistivity measurements were made using the single crystal, four-probe method. A typical crystal of dimensions $0.15 \text{ mm} \times 0.15 \text{ mm} \times 2.0 \text{ mm}$ was mounted with ultrasonic indium solder to four gold leads along the needle axis (b axis). Initially, conducting silver epoxy was used for contacts, but these were found to react (perhaps $Ag^+ \leftrightarrow Cu^+$ ion exchange with the crystal) and the contact resistance became quite large after several hours. The room-temperature resistance of the crystal was measured as 0.24Ω . The distance between the two voltage contacts measured approximately 1 mm, and hence, the room-temperature resistivity can be calculated to be $5 \times 10^{-4} \Omega \text{ cm}$. An uncertainty of $\pm 30\%$ is estimated from the size of the contacts and the irregular crystal shape. The crystal exhibited ohmic behavior at room temperature, as well as stability of the contact resistance over the course of days.

Temperature dependence of the observed resistance of

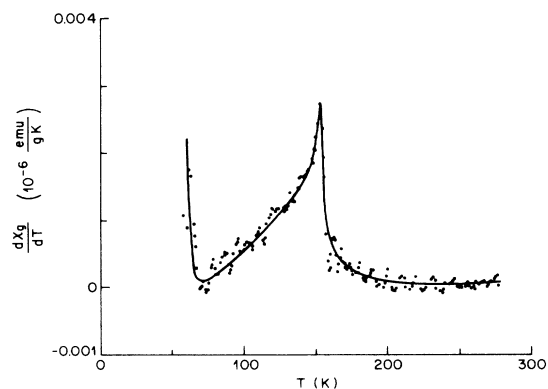


FIG. 4. Magnetic susceptibility derivative dX_g/dT obtained by numerically differentiating the corrected susceptibility. The peak at $152 \pm 1 \text{ K}$ indicates a second-order, reversible transition.

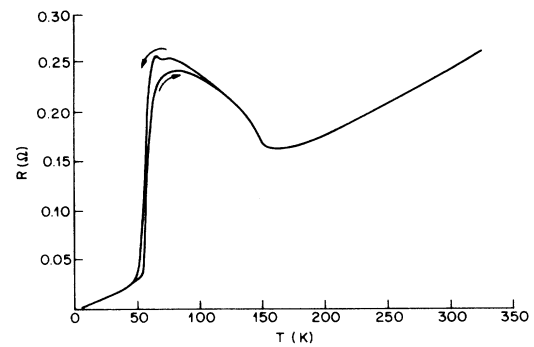


FIG. 5. Temperature dependence of the experimentally observed resistance for a single crystal of $K_3Cu_8S_6$. The room-temperature resistance of 0.24Ω corresponds to a resistivity of $5 \times 10^{-4} \Omega \text{ cm}$ ($\pm 30\%$).

the crystal is plotted in Fig. 5 for the range 5–350 K. The resistance decreases with decreasing temperature, indicative of metallic behavior down to about 160 K. There is a reversible phase transition at about 150 K which corresponds well with the phase transition observed at $152 \pm 1 \text{ K}$ in the magnetic susceptibility. Upon further cooling, the resistance rises until about 63 K, where there is a small dip in the resistance, just as there is in the magnetic susceptibility. Further cooling shows a dramatic decrease in resistance and leads to a state which is again metallic in the region of 5–50 K. The heating curve demonstrates that a considerable hysteresis exists and that it extends up to at least 100 K. As in the case of the magnetic susceptibility, the heating curve does not display the anomaly near 63 K. Figure 6 shows dR/dT versus temperature and again show that the second-order phase transition occurs at about 152 K. As in the case of the magnetic susceptibility, the derivative was obtained by fitting the experimental data to a quadratic polynomial for every eight consecutive points, and extracting the linear coefficient as the slope.

C. Specific heat

The specific heat of $K_3Cu_8S_6$ was measured¹⁰ in the temperature range of 100 K to 300 K. The specific heat

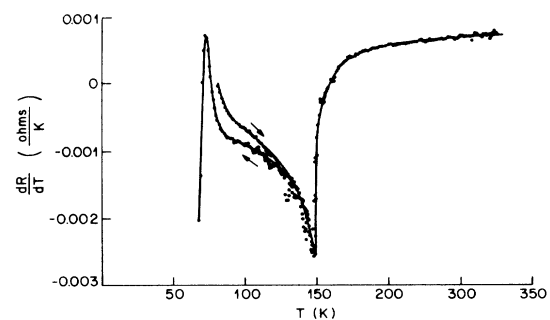


FIG. 6. The derivative dR/dT plotted as a function of temperature demonstrates the existence of the second-order phase transition at 153 K as well as the broad hysteresis due to the first-order transition.

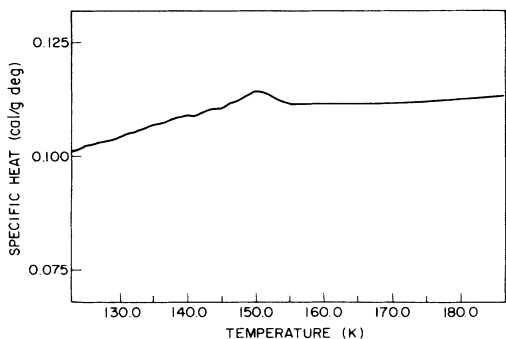


FIG. 7. Specific-heat data for $K_3Cu_8S_6$ display a reversible anomaly near 150 K.

shows no unusual behavior down to 160 K, and is almost constant. As shown in Fig. 7, there is a small peak in the region of 150 K, and both heating and cooling runs gave the same curve. This corresponds to the reversible phase transition seen in both the magnetic susceptibility and the electrical resistivity. The slope of the specific heat is more positive below the transition region than it is above the transition region.

IV. DISCUSSION

A relatively large number of copper-sulfide phases are known and most contain discrete oxidation (valence) states.⁴ The major exception is the $Cu_{2-x}S$ ($0 \leq x \leq 0.2$) binary system where a variety of nonstoichiometric, "mixed-valence" phases can be found. An additional exception lies in the K-Cu-S system, of which $K_3Cu_8S_6$, KCu_4S_3 , and KCu_3S_2 are members, but only $K_3Cu_8S_6$ and KCu_4S_3 provide mixed-valence examples.

Although it is tempting to describe copper-sulfur mixed-valence compounds as $Cu^I Cu^{II}$ systems, most of the available evidence suggests that the mixed-valency resides primarily on the sulfur and not on the copper.¹¹⁻¹³ X-ray photoelectron spectroscopy suggests that all known copper sulfides (including $Cu_{2-x}S$, KCu_4S_3 , and $Na_3Cu_4S_4$) contain only Cu(I). There is no direct evidence to date that shows that Cu(II) or intermediate oxidation states exist in these copper-sulfide phases. With these results in mind, the mixed-valency in KCu_4S_3 might be formulated as $K^+Cu_4^+(S^{2-})_2S^-$. Similarly, another example is provided by $Na_3^+Cu_4^+(S^{2-})_3S^-$ in $Na_3Cu_4S_4$. As such, we can formulate $K_3Cu_8S_6$ as a Robin-and-Day¹⁴ class IIIB mixed-valence material with the formula $K_3^+Cu_8^+(S^{2-})_5S^-$. These ionic-like notations are useful primarily for descriptive purposes and are consistent with results from photoelectron spectroscopy of copper sulfides. However, it is clear that covalency is very important in these phases, and it is likely that the wave functions at the Fermi surface of these metallic compounds have considerable copper as well as sulfur character.

As a class IIIB mixed valence material, $K_3Cu_8S_6$ could be expected to show metallic behavior. The electrical resistivity results confirm this with a drop in resistivity of

approximately two orders of magnitude from 300 to 5 K. The absolute value of the resistivity [ρ (300 K) $\cong 5 \times 10^{-4} \Omega \text{ cm}$] is similar in value to other metallic phases with layered structures.¹⁵

From a structural point of view, $K_3Cu_8S_6$ is also an interesting material. The crystal structures of KCu_4S_3 , $K_3Cu_8S_6$, and KCu_3S_2 are shown in Fig. 8. The low-temperature phase KCu_4S_3 is a close-packed double-layered structure (S-Cu-S-Cu-S) in which all copper ions are tetrahedrally coordinated.⁴ The high-temperature phase, KCu_3S_2 , is also a layered structure but has a pleated character because the copper ions are in both tetrahedral and trigonal coordination sites.⁶ A remarkable feature of KCu_3S_2 is that one-dimensional chains of $[Cu_4S_4]^{n-}$ of infinite length, which we will denote by ${}_{\infty}^1[Cu_4S_4]^{n-}$, are bridged by edge-sharing tetrahedra to

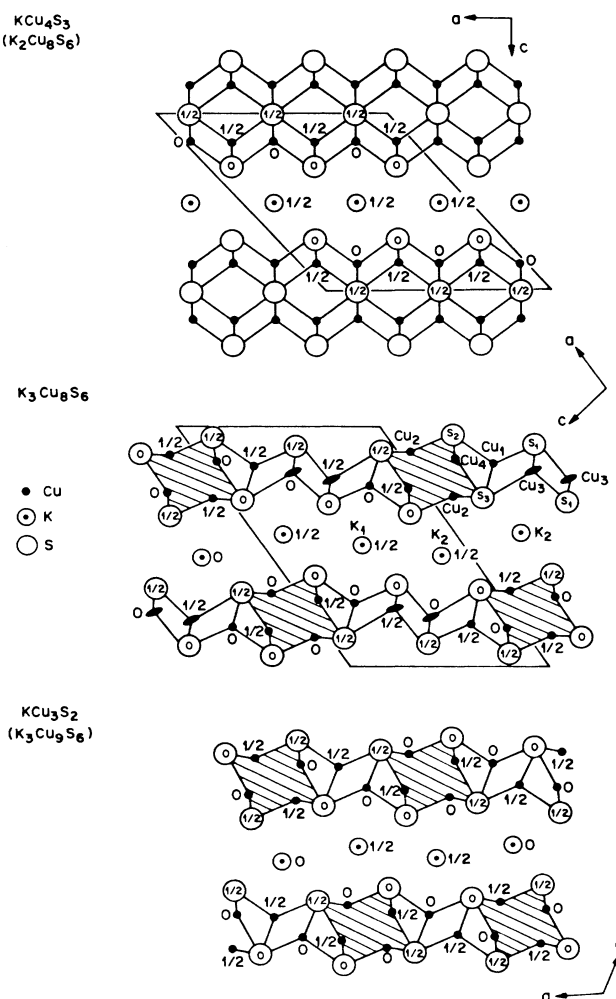


FIG. 8. Representations of the structures of KCu_4S_3 , $K_3Cu_8S_6$, and KCu_3S_2 . In $K_3Cu_8S_6$, note how Cu(1), Cu(3), S(1), and S(3) form a small segment of half of the double layer found in KCu_4S_3 , while Cu(2), Cu(4), S(2), and S(3) form the ${}_{\infty}^1[Cu_4S_4]^{n-}$ component of the layered structure. In all cases, the potassium ions separate the layered structures.

yield the pleated layers, which are separated by potassium ions. The structure of $K_3Cu_8S_6$ is intermediate between that of KCu_4S_3 and KCu_3S_2 .⁷ It is not surprising then that the $K_3Cu_8S_6$ synthesis conditions are "intermediate" between the syntheses of KCu_4S_3 and KCu_3S_2 . Additionally, the stoichiometric sequence



also suggests that $K_3Cu_8S_6$ might be an intermediate structure.

$K_3Cu_8S_6$ is most like KCu_3S_2 in that the ${}^1_{\infty}[Cu_4S_4]^{n-}$ chain is an integral part of the layer structure. Figure 9 schematically demonstrates how this vital part of $K_3Cu_8S_6$ is based upon trigonal coordination of the copper ions. These resultant ${}^1_{\infty}[Cu_4S_4]^{n-}$ chains are bonded into layers using edge-sharing tetrahedra that resemble a small segment of half of the double layer found in the KCu_4S_3 structure. The crystal structure report by Burschka shows that the Cu3 ions, which are the heart of this bridging network between ${}^1_{\infty}[Cu_4S_4]^{n-}$ chains, have either a large amount of thermal motion or a slight disorder.⁷ (This is indicated in Fig. 8 by the elliptical shapes assigned to the Cu3 ions.) It is interesting to note at this point that the idea of a ${}^1_{\infty}[M_4S_4]^{n-}$ chain is also evident in other structures. Figure 10 demonstrates that $Na_3Cu_4S_4$ and $K_2Ag_4S_3$ also possess this columnar chain as the fundamental unit of their solid-state structure. It is clearly the manner in which this columnar chain packs into the lattice that is responsible for the overall differences in structure. In the case of $K_3Cu_8S_6$ (as well as the others) the packing of these ${}^1_{\infty}[Cu_4S_4]^{n-}$ chains into layers results in layers which have an anisotropic character, unlike the more conventional layered materials such as $NbSe_2$, TaS_2 , etc.

The electrical resistivity and magnetic susceptibility for $K_3Cu_8S_6$ clearly show the presence of phase transitions in the region of 55 and 150 K. The most likely explanation for the observed behavior in $K_3Cu_8S_6$ is the presence of a charge-density wave (CDW). Charge-density waves are most common in lower-dimensional materials (metals) such as $NbSe_3$ (one-dimensional) and $TaSe_2$ (two-

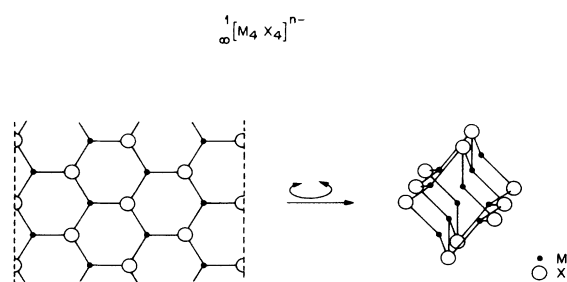


FIG. 9. Schematic representation of how the vital ${}^1_{\infty}[Cu_4S_4]^{n-}$ structure is obtained from trigonally coordinated cooper ions. The sheet of trigonally coordinated copper on the left is wrapped around (so that dashed lines meet) to yield the columnar chain structure on the right.

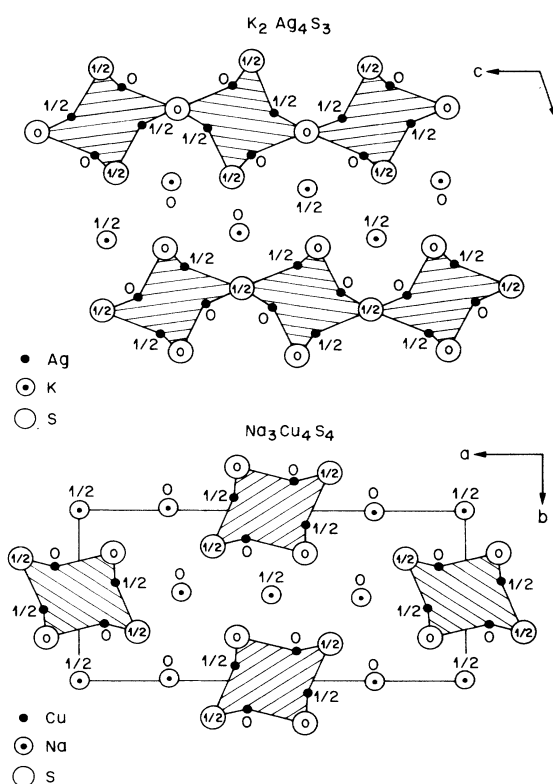


FIG. 10. Structures for $Na_3Cu_4S_4$ and $K_2Ag_4S_3$. The views down the b axes (${}^1_{\infty}[Cu_4S_4]^{n-}$ chain axis) demonstrate the similarity to the K-Cu-S systems.

dimensional) but are occasionally seen in three-dimensional materials such as CuV_2S_4 .¹⁶ The simplest models suggest that CDW formation is favored in low-dimensional metals because anisotropic Fermi surfaces with regions of low curvature are expected to occur, while in three-dimensional materials such occurrences are "accidental."¹⁷ $K_3Cu_8S_6$ is clearly a lower-dimensional metal. However, the layers of $K_3Cu_8S_6$ have an anisotropic two-dimensional character because of the manner in which the layers are composed of chains. The crystal dimensions were too small to obtain a measure of the electrical in-layer anisotropy, but the retention of metallic behavior below the transitions suggests that the anisotropy is not large enough to make the system quasi-one-dimensional. Such large anisotropies do exist in some structurally two-dimensional metals so that the CDW properties are effectively one dimensional (for example, in $K_{0.3}MoO_3$).¹⁸ Since $K_3Cu_8S_6$ meets the structural criteria and can be considered a low-dimensional metal, CDW formation is a likely explanation for the observed magnetic susceptibility and electrical resistivity based on the similar behavior of precedent systems.¹⁷ In particular, the observed behavior of $K_3Cu_8S_6$ is very similar to CuV_2S_4 .¹⁶ The major difference is the enhanced value of the magnetic susceptibility in CuV_2S_4 due to electron-electron interactions, as well as the actual temperatures of the transitions. The magnitude of the relative behavior in terms of

changes in susceptibility at the phase transitions is, however, very similar between $K_3Cu_8S_6$ and CuV_2S_4 . However, observation of an incommensurate lattice modulation in a metal is what is really needed in order to show CDW formation. Our preliminary low-temperature single-crystal x-ray diffraction results do indeed indicate that the phase transition at 153 K produces an incommensurate state with a wave vector $\mathbf{q}=(1-\delta)\mathbf{b}^*/2$ where $\delta(150\text{ K})\simeq 0.1$ (note that \mathbf{b}^* is parallel to \mathbf{b} , which lies along the needle axis). The distortion becomes commensurate at the first-order transition near 55 K. This structural data coupled with the physical properties strongly suggest CDW formation in $K_3Cu_8S_6$. Further x-ray work is in progress and will be reported later.

V. CONCLUSION

We have refined and explained the previously confusing synthesis of the interesting structure $K_3Cu_8S_6$. Based on

structural similarities to KCu_4S_3 and KCu_3S_2 , we conclude that $K_3Cu_8S_6$ is a kinetic phase which must be carefully "trapped." Investigation of the electrical resistivity and magnetic susceptibility has led us to suggest that CDW formation is responsible for the phase transitions in $K_3Cu_8S_6$. Based on the mixed valency (e.g., metallic properties) and the low-dimensional structure of $K_3Cu_8S_6$, CDW formation is indeed likely. X-ray results confirm the presence of an incommensurate lattice below 150 K. Future results will be reported on in order to structurally describe the CDW phenomena in $K_3Cu_8S_6$.

ACKNOWLEDGMENTS

We would like to acknowledge our former colleague, D. B. Brown, who originally brought the K-Cu-S systems to our attention.

*Present address: Department of Chemistry, Baker Laboratory, Cornell University, Ithaca, New York 14853.

¹W. Rudorff, H. G. Schwarz, and M. Walter, *Z. Anorg. Allg. Chemie* **269**, 141 (1952).

²C. Burschka, *Z. Naturforsch.* **346**, 396 (1979).

³Z. Peplinski, D. B. Brown, T. Watt, W. E. Hatfield, and P. Day, *Inorg. Chem.* **21**, 1752 (1982).

⁴D. B. Brown, J. A. Zubieta, P. A. Vella, J. T. Wroblewski, T. Watt, W. E. Hatfield, and P. Day, *Inorg. Chem.* **19**, 1945 (1980).

⁵C. Burschka, *Z. Anorg. Allg. Chem.* **463**, 65 (1980).

⁶C. Burschka and W. Bronger, *Z. Naturforsch.* **326**, 11 (1977).

⁷C. Burschka, *Z. Naturforsch.* **34B**, 675 (1979).

⁸H. Schils and W. Bronger, *Z. Anorg. Allg. Chemie* **456**, 187 (1979).

⁹F. J. Di Salvo, S. A. Safran, R. C. Haddon and J. V. Waszczak, *Phys. Rev. B* **20**, 4883 (1979).

¹⁰F. S. Bates, H. E. Bair, and M. A. Hartney, *Macromolecules* **17**, 1987 (1984).

¹¹J. C. W. Folmer, Ph.D. thesis, University of Groningen, 1981.

¹²J. C. W. Folmer and F. Jelinek, *J. Less-Common Met.* **76**, 153 (1980).

¹³C. F. van Bruggen, *Ann. Chim. Fr.* **7**, 171 (1982).

¹⁴M. B. Robin and P. Day, *Adv. Inorg. Chem. Radiochem.* **10**, 248 (1967).

¹⁵See for example, F. J. Di Salvo, and T. M. Rice, in *Phys. Today*, **32**, 32 (1979).

¹⁶R. M. Fleming, F. J. Di Salvo, R. J. Cava, and J. V. Waszczak, *Phys. Rev. B* **24**, 2850 (1981).

¹⁷F. J. Di Salvo, in *Electron-Phonon Interactions and Phase Transitions*, edited by T. Riste (Plenum, New York, 1977), p. 107.

¹⁸L. F. Schneemeyer, F. J. Di Salvo, R. M. Fleming, and J. V. Waszczak, *J. Solid State Chem.* **54**, 358 (1984).